

Geophysical Research Letters[®]



RESEARCH LETTER

10.1029/2024GL110554

Key Points:

- Accompanying optical pulse is subsequent to TGF
- TGF precedes the current surge in the leader channel and cannot be generated by this current surge
- TGF may be terminated by the current surge in the leader channel

Correspondence to:

A. Mezentsev,
Andrey.Mezentsev@uib.no

Citation:

Mezentsev, A., Østgaard, N., Marisaldi, M., Sarria, D., Lehtinen, N., Neubert, T., et al. (2024). Discerning TGF and leader current pulse in ASIM observation.

Geophysical Research Letters, 51, e2024GL110554. <https://doi.org/10.1029/2024GL110554>

Received 4 JUN 2024
Accepted 31 OCT 2024

Discerning TGF and Leader Current Pulse in ASIM Observation

A. Mezentsev¹ , N. Østgaard¹ , M. Marisaldi¹ , D. Sarria¹ , N. Lehtinen¹ , T. Neubert² , O. Chanrion² , and F. Gordillo-Vazquez³

¹Department of Physics and Technology, University of Bergen, Bergen, Norway, ²National Space Institute, Technical University of Denmark, Kongens Lyngby, Denmark, ³Instituto de Astrofísica de Andalucía, CSIC, Granada, Spain

Abstract Terrestrial gamma ray flash (TGF) observations made by the Atmosphere-Space Interaction Monitor (ASIM) have demonstrated that these TGFs are accompanied by a prominent optical pulse from a hot leader channel. It is hard to confidently resolve the true sequence of the events in the source region due to temporal proximity of the involved processes. Here we report a bright long duration TGF together with its associated optical recordings showing clear temporal separation between the TGF and the optical pulse. In this observation the optical pulse is clearly distinct and subsequent relative to the TGF. The corresponding lightning discharge occurred at the very end of the TGF. We conclude that the current surge inside the lightning leader channel cannot be responsible for generation of this TGF. The current surge that produced the associated optical pulse can itself be conditioned by the TGF and may be responsible for the TGF termination.

Plain Language Summary TGFs observed from space are found to be associated with current surges in lightning leader channels. These current surges emit radio waves and can be detected with lightning detection networks. They also produce optical pulses which can be observed by the optical sensors on board of the space satellites. The fact that TGFs have usually short duration does not allow to define the real sequence of events in the source region due to timing uncertainties. In this paper we report a unique observation of a rare coincidence of a long duration TGF accompanied by an optical pulse and a high peak current lightning detection. Duration of the TGF is one order of magnitude larger than the overall observational uncertainty, which allows us to reliably discern the TGF and the accompanying current pulse in the leader channel. We could confidently conclude that the TGF was generated first, in the very end of the TGF the current surge in the leader channel occurred, and the optical pulse was produced. The appearance of the current surge close to the end of the TGF can indicate that the current surge is conditioned by the TGF, and, reciprocally, it could condition the TGF termination.

1. Introduction

Terrestrial gamma ray flashes (TGFs) being the bursts of high energy photons shot from Earth's atmosphere to space, are known to be produced during the initial upward propagation of the +IC lightning leader (Cummer et al., 2011, 2015; Lu et al., 2010; Shao et al., 2010; Skeie et al., 2022; Østgaard et al., 2013, 2021). Very low frequency (VLF) and low frequency (LF) radio sferics can often be found in association with short duration TGFs (Connaughton et al., 2013; Dwyer & Cummer, 2013; Mezentsev et al., 2018).

The Atmosphere-Space Interactions Monitor (ASIM) provides synchronous X- (low energy detector (LED)) and gamma ray (high energy detector (HED)) measurements (modular X- and gamma ray sensor (MXGS)) with optical recordings in ultra-violet (UV) band 180–240 nm, 337 nm (blue) and 777.4 nm (red) wavelength (modular multispectral imaging array (MMIA)). They allow for synchronous detection of TGFs and optical signals associated to related lightning processes, as MXGS and MMIA modules are synchronized down to $\pm 5 \mu\text{s}$.

ASIM observations since 2018 have shown that TGFs within the field of view (FOV) of the optical instruments are accompanied by a prominent optical pulse (Skeie et al., 2022; Østgaard et al., 2019) in the beginning of a lightning flash (Lindanger et al., 2022). This optical pulse, associated with the TGF, manifests itself at both, 337 and 777.4 nm optical channels. The emission at 777.4 nm corresponds to the atomic oxygen emission line OI (Chanrion et al., 2019), which requires hot plasma in the lightning leader channel. The 337 nm emission corresponds to the second positive system N₂P of the molecular nitrogen (Chanrion et al., 2019), which is excited by the electron impact and corresponds to the cold streamer plasma.

TGFs observed by ASIM have a clear tendency to slightly precede the optical pulse associated with them (Skeie et al., 2022; Østgaard et al., 2019), but the short duration of TGFs combined with the uncertainty introduced by the optical delay of the lightning light propagating through the cloud (Luque et al., 2020) do not allow us to confidently resolve the true sequence of these events (Østgaard et al., 2021). The same problem is present in the radio measurements: the TGF current is usually mixed with the lightning current in the recordings due to temporal proximity of the involved processes, which makes it difficult to discern the TGF source current in the radio measurements (Østgaard et al., 2021).

In this contribution we report a remarkable TGF with high fluence and long duration (580 μ s) together with its associated optical recordings which show clear distinction between the TGF and the optical pulse. A Global Lightning Detection network (GLD360) detection, that corresponds to the current surge in the +IC leader channel and the associated optical pulse, occurred at the very end of this TGF, which can refer to a possibility for this current surge to terminate the TGF. The long duration of this TGF helps to establish the temporal sequence of events at the source region and test several possible scenarios of causative relations between TGFs and their related IC lightning processes.

Presented observations, results and conclusions are relevant only to the upward TGFs produced by +IC lightning leaders. One should not try to generalize these results and expand them onto the downward TGFs and associated CG discharges, due to essentially different generation conditions of these two classes of TGFs.

2. Observation

On 3 December 2021, at 21:15:39.405,400 UTC the ASIM MXGS observed a bright and long duration TGF. The HED unit has registered 360 counts with an overall duration of the event of 580 μ s. That was an extraordinary event, as 80% of ASIM TGFs have HED fluence less than 100 counts, 95% exhibit fluence less than 200 counts, and only 0.7% of all ASIM TGFs have a fluence higher than 360 counts.

At the moment of the TGF detection ASIM was passing right over an active cell of an equatorial thunderstorm over Central Africa. Figure 1 shows the ISS trajectory with the ASIM position at the trigger time as a magenta dot. The lightning activity context is represented by Worldwide Lightning Location Network (WWLLN) detections within $\pm 1,000$ s around the trigger time and is shown by the black dots in the inset overview map. The main panel shows the MMIA image projected onto the 15 km altitude above the Earth surface (assumed cloud top altitude), with the superimposed ISS trajectory (black line), the ASIM footprint at the trigger time (magenta dot), GLD360 detections during 665.6 ms of the ASIM optical trigger (red dots) with their error ellipses (green), and the GLD360 detection associated with the TGF (red dot with black error ellipse). The spatial scale of 10 km is represented by the white L-shape mark in the lower corner of the MMIA image.

The TGF itself is presented in Figure 2. The upper panel combines the scatter plots for the HED and LED units, showing individual photon counts' energies versus detection time. The large amount of photons with energies above 10 MeV (with highest energies up to 23 MeV) and the sharp ending of the TGF without a prominent Compton tail in HED are indicative of ASIM being inside the TGF emission cone (Bjørge-Engeland et al., 2022; Hazelton et al., 2009; Skeie et al., 2022), which puts the TGF source well inside the FOV of the ASIM optical instruments, and confirms close association of the TGF and the subsequent optical pulse (Figure 2, lower panel). The lower panel shows combined lightcurves of the TGF in the HED and LED units, and lightcurves of the 337 and 777.4 nm (blue and red) photometer recordings. The prominent optical pulses in both, blue and red channels, start rising straight after what looks like an abrupt termination of the TGF. The GLD360 detection associated with the TGF is shown with ± 50 μ s uncertainty as a black dashed line inside the magenta bar (radio signal propagation time between the source and the ISS is accounted for), see details below.

The context of the optical activity around the time of the TGF in the blue and red optical channels is shown in Figure 3. Two upper panels show camera images and photometric recordings for the 337 nm channel (blue), and two lower panels correspond to the 777.4 nm (red) photometer and camera recordings. The photometric recordings represent accumulated light from the whole FOV in a specific channel, sampled at 100 kHz (each sample is 10 μ s), showing evolution of the optical signals on a sub-millisecond time scale. The camera images have the time exposure of 83.2 ms for each frame, but they provide a high spatial resolution of about 400 \times 400 m for a pixel (at the center of the FOV). The photometric recordings are split into separate frames for convenience according to the cameras' frames.

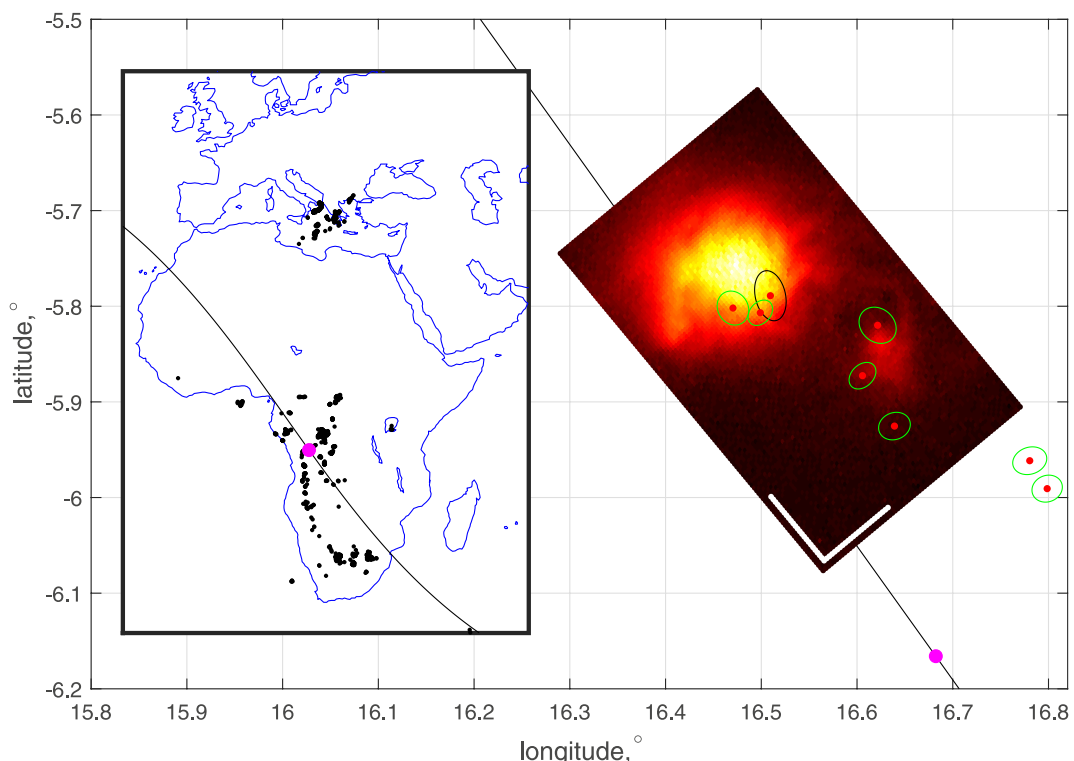


Figure 1. Context map. The main panel shows the ISS trajectory (black line) and the footprint (magenta dot), the MMIA 83 ms long image of the lightning activity in 337 nm, GLD360 detections during the MMIA observation (red dots with green error ellipses), GLD360 detection associated with the TGF termination (red dot with black error ellipse); white mark in the lower corner of the MMIA image refers to a spatial length of 10 km. The inset shows the ISS trajectory and the contextual lightning activity given by the WWLLN (black dots).

The blue and red image panels (Figure 3) show consistently two separate sources of activity: in the lower and in the upper halves of the frame. The bright big spot in the upper half of the frame #4 represents the bright optical pulse associated with the TGF in both channels, and likely shows the spatial location of the TGF source. There are no other optical signals within the FOV of the ASIM optical instruments during the considered 665.6 ms of the MMIA observation around the TGF time, so, given that ASIM was within the TGF emission cone, we can confidently attribute the optical source location (consistent with the GLD360 source location, see Figure 1) to the TGF source location.

ASIM has poor absolute timing due to peculiarities of its hardware architecture, which results in the absolute timing of each trigger to have an unknown random uncertainty within 0–40 ms. This makes it hard to coordinate ASIM measurements and other instruments' recordings with high temporal accuracy, and requires some additional cross-platform analysis to mitigate this uncertainty. At the same time ASIM has a $\pm 5 \mu\text{s}$ relative timing accuracy between MXGS and MMIA, and the state of the MMIA timer at every reset (every second) is recorded together with each trigger. This allows us to extrapolate the known reference time through the data (in the case when a precise time reference has been obtained somehow) for the data segments without long (greater than 1 s) data gaps. In our case we managed to time-tag the ASIM data and position the GLD360 detection at the very end of the TGF, as shown in Figure 4.

The reconstruction of the absolute timing with a precision of $\pm 50 \mu\text{s}$ was possible due to a detection of an Elve event 8.745 s after the TGF, shown in Figure 5. The Elve was generated by a negative cloud to ground (-CG) discharge with a peak current of -82 kA (according to GLD360) detected at 21:15:48.149 UTC by GLD360 at about 123 km off the ISS footprint. The electromagnetic pulse (EMP) from the -CG return stroke hits the ionosphere and excites an Elve, whose UV emissions propagate further and are detected by the ASIM UV photometer. The parent EMP does not experience any cloud moderation, which results in the Elve lightcurve to reach its peak earlier compared to the blue and red optical pulses, delayed due to cloud scattering (Figure 5).

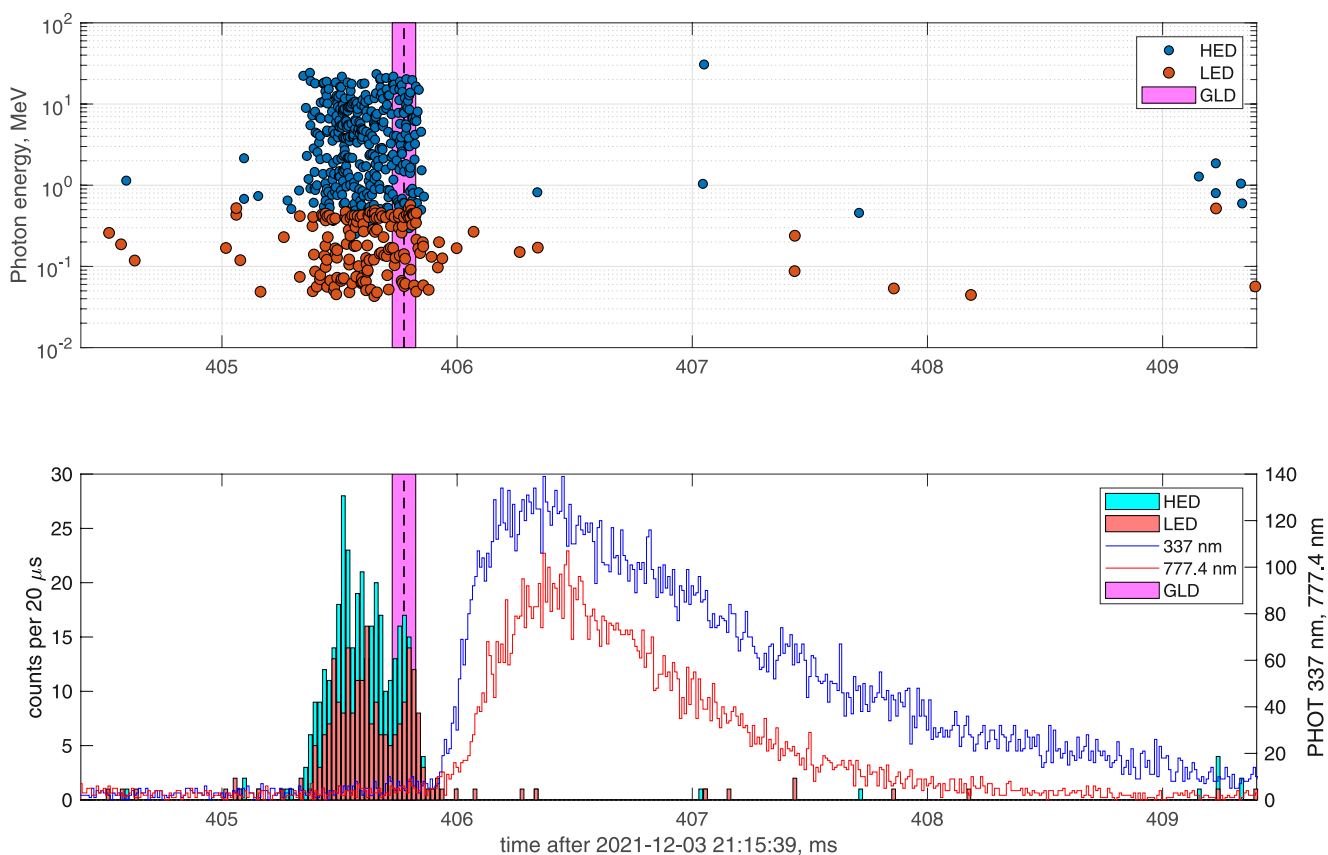


Figure 2. TGF, optical observation, and GLD360 detection. Upper panel: counts' energies versus time measured by HED (blue circles) and LED (red circles); the GLD360 detection associated with the TGF termination stage is given by the vertical black dashed line with time uncertainties (magenta bar). Lower panel: HED (cyan bars) and LED (red bars) TGF lightcurve versus time with concurrent optical measurements in 337 nm (blue line) and 777.4 nm (red line); the GLD360 detection is shown the same way as in the upper panel.

We use then the onset of the UV Elve lightcurve (defined with $\pm 50 \mu\text{s}$ accuracy) as the moment of the parent EMP arrival at ASIM. Thus, the time of the GLD360 detection increased by the light propagation time between the source and the ASIM position, is linked to the UV Elve lightcurve onset and serves as the absolute time reference. Given that there were no long data gaps between the TGF-related and Elve-related MMIA recordings, it was possible to extrapolate this absolute time reference onto the TGF observation. Notice that the use of a combination of an MMIA recording of a regular lightning with its parent GLD360 detection gives an absolute time reference with an accuracy of the order of 1 ms only, which could not allow us to position the GLD360 detection precisely during the TGF event.

3. Discussion

Previous ASIM observations (Skeie et al., 2022; Østgaard et al., 2019; Østgaard et al., 2021) clearly showed that ASIM TGFs are accompanied by a strong optical pulse in 777.4 nm, attributed to a current surge in the +IC leader channel. ASIM TGFs have a tendency to slightly precede the associated optical pulse (Skeie et al., 2022; Østgaard et al., 2019), and these TGFs are also reported to occur during the initial stage of a lightning flash (Lindanger et al., 2022). Short characteristic TGF core duration of about 100 μs (Bjørge-Engeland et al., 2022; Skeie et al., 2022) makes it impossible to confidently discern the TGF and the associated optical pulse (with characteristic rise time of 200–500 μs), and reveal their true sequence at the source region. However, we are able to suggest several scenarios regarding their possible interrelation due to systematically observed close time association between ASIM TGFs and their related optical pulses.

According to all previous ASIM observations, a strong current surge occurs in a leader channel either during, or shortly after a TGF. This can be realized in a few different ways.

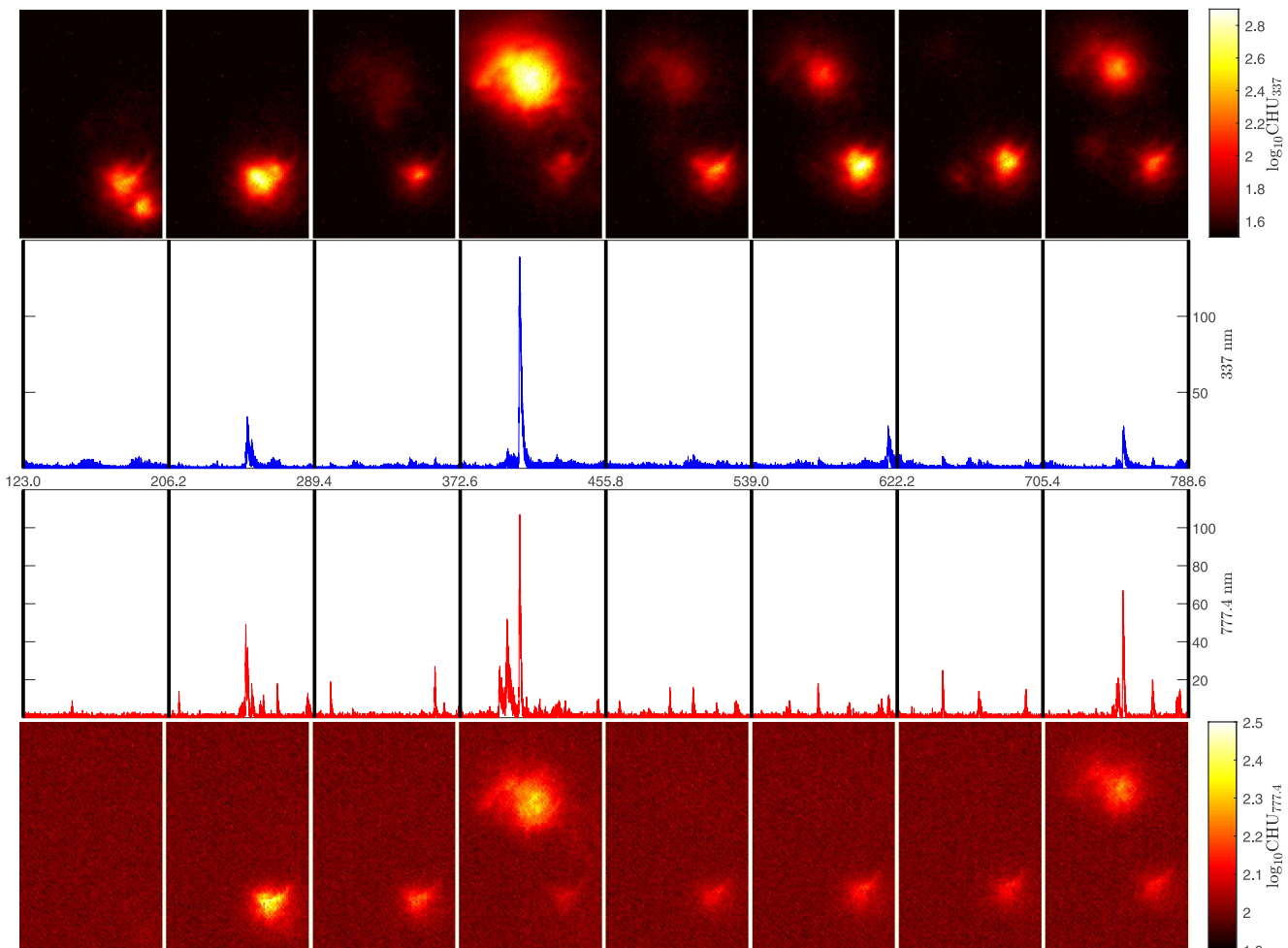


Figure 3. Contextual optical activity around the TGF observation in the blue and red optical channels, 337 and 777.4 nm correspondingly. Two upper panels: camera images and photometric recordings for the 337 nm channel. Two lower panels: photometric recordings and camera images for the 777.4 nm channel. Frames' time boundaries are marked with ms after 21:15:39 UTC.

1. A TGF is produced by the current surge in the leader channel, such that the current surge creates conditions for the TGF generation;
2. A TGF evolves concurrently, but independently from the current surge in the leader channel, such that the TGF coexists with the current through the leader channel, but is not conditioned by this current. The causative relation may be deeper in this case: both, the current surge and the TGF are conditioned by the same cause;
3. A TGF precedes the current surge in the leader channel and, possibly, facilitates the occurrence of this current surge;
4. A TGF precedes the current surge in the leader channel and is terminated by it, such that the current surge destroys conditions for the TGF generation.

One of the crucial problems in revealing the sequential order between a TGF and accompanying lightning activity is that TGFs have short characteristic core duration, while the optical pulses exhibit much longer characteristic rise times and experience a certain delay due to cloud scattering. This circumstance makes it difficult to pinpoint a short process relative to a much longer process given the uncertainties due to cloud scattering. With the reported event we can solve this problem. The uniqueness of this observation is in the coincidence of the long core duration of the TGF (twice as long as the rise time of the accompanying optical pulse) and the fortunate observation geometry with ASIM being inside the TGF emission cone. In addition, the Elve detection (not related to the TGF) allowed us to pinpoint the TGF on the absolute time axis and position the GLD360 detection relative to the TGF with high accuracy of $\pm 50 \mu\text{s}$.

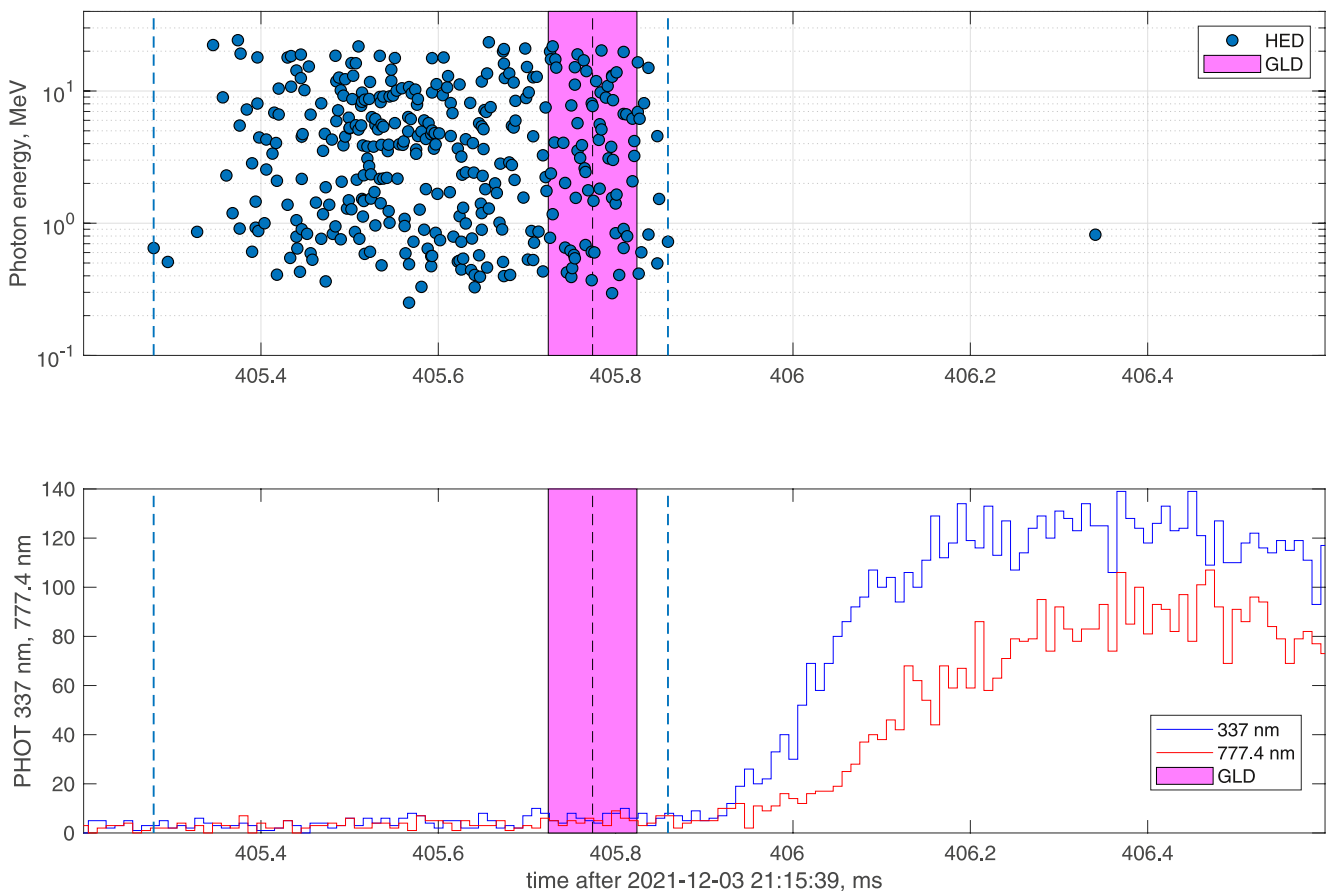


Figure 4. Transition zone from the TGF to the optical pulse. Upper panel: counts' energies measured by HED (blue circles) versus time, GLD360 detection (black vertical dashed line) and its time uncertainty (magenta bar) during the TGF termination stage, TGF time boundaries (blue vertical dashed lines). Lower panel: GLD360 detection and TGF boundaries, same as on the upper panel, optical photometric recordings in 337 nm (blue line) and 777.4 nm (red line).

This observation clearly shows that this particular TGF appears and evolves through its life cycle before the current surge in the leader channel occurs. This allows us to rule out the current surge in the leader channel from the list of possible mechanisms responsible for conditioning the TGF generation. We can confidently say that it is not the current surge in the leader channel that generates this TGF.

The TGF termination coincides with the current surge in the leader channel as given by the GLD360 detection (see the zoomed transition zone in Figure 4). The delay between the GLD360 detection and the onset of the optical pulse related to this current surge is due to scattering and propagation through the cloud, and constitutes about 150–200 μ s, which is a typical value for this type of discharge (Luque et al., 2020; Østgaard et al., 2021).

The appearance of the current surge (GLD360 detection) close in time to the TGF termination stage may reflect twofold, reciprocal connection between the TGF and the current surge in the leader channel. Clear sequential order between the TGF and the associated optical pulse, systematically found as a tendency in the earlier ASIM observations, and revealed clearly in this particular observation, indicates that TGF can be the process that conditions and facilitates subsequent current surge in the leader channel. In turn, the current surge itself can be responsible for the TGF termination, or be a manifestation of the conditions leading to the TGF termination.

Our previous work (Skeie et al., 2022) has shown that the common feature for all TGFs from within the FOV of MMIA with concurrent optical measurements is that the associated optical pulse does not precede the onset of a TGF: TGFs are sitting on the beginning of the rising edge of the optical pulse, or before it. Given the uncertainties, this suggests certain uniformity for the TGF to current surge relation. It is also hard to suggest the existence of two essentially different mechanisms of TGF generation for TGFs of the same type: before the current surge and after the current surge, because they correspond to the two drastically different sets of conditions on the ambient

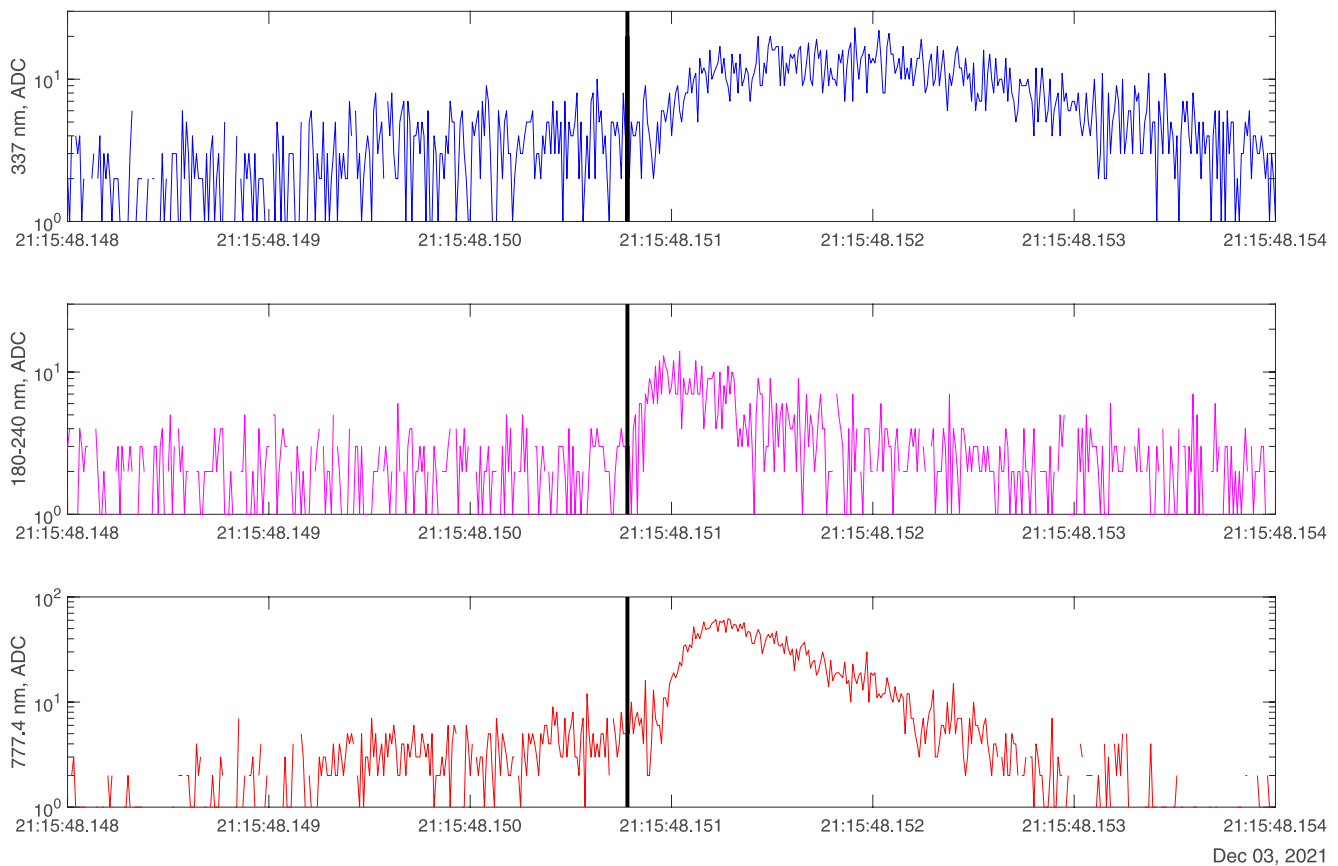


Figure 5. Photometric recordings of a -CG discharge in 337 nm (upper panel, blue line) and 777.4 nm (lower panel, red line), parent to the Elve event (middle panel, magenta curve). The GLD360 detection (vertical black line) of the -CG return stroke was attributed to the onset of the Elve (see text for details).

electric field. Thus, the uniformity of the observations and the uniformity of the events have to suggest also the uniformity in generation conditions, and there is at least one numerous class of TGFs that shares this mechanism, where a TGF is followed (and potentially terminated) by a current surge in the +IC leader channel.

One of the possible scenarios of a TGF generation in the context of a subsequent current surge in the leader channel could be the following. During the initial stage of the +IC leader development the electric field grows above the TGF generation threshold and a TGF gets generated. The leader development continues and results (potentially with a contribution from the TGF) in a current surge in the channel, which collapses the field in the TGF generation zone, and the TGF terminates. What type of processes cause the appearance of the current surge in the leader channel we cannot say based on our observations. Clarification of this moment requires a new set of modeling efforts within the proposed framework, and further observations with more advanced instrumentation.

4. Conclusion

We have presented a unique observation of a TGF, which combines unusually long TGF core duration with favorable observation geometry due to ASIM being inside the TGF emission cone. Concurrent optical recordings show that the onset of the accompanying optical pulse in both blue (337 nm, streamers) and red (777.4 nm, leader) channels is clearly subsequent to the TGF, and occurs a few tens of microseconds after the TGF termination. Long TGF core duration of $580 \mu\text{s}$ is twice as long as the optical rise time, which allows us to exclude the influence of possible uncertainties due to cloud scattering, and reveal the true sequential order of the events at source.

This observation is supported by a GLD360 detection corresponding to the optical pulse and representing the current surge in the +IC leader channel. Refined absolute timing due to an Elve observed shortly after the TGF allowed us to position the GLD360 detection at the very end of the TGF. Such a relation can refer to this current surge as a possible cause of the TGF termination.

We have demonstrated that this TGF clearly precedes the current surge in the leader channel, which allows us to rule out this current surge from possible mechanisms responsible for generation of this TGF. On the contrary, the current surge in the leader channel may condition the TGF termination via collapsing electrical field in the TGF generation zone.

Data Availability Statement

All ASIM data are available at the ASIM Data Center (<https://asdc.space.dtu.dk/>). All questions related to the ASIM data processing should be addressed to the ASIM science team. The data used to produce the figures in this paper (except for WWLLN data, which is commercial) are uploaded to Zenodo and available at <https://doi.org/10.5281/zenodo.11394750> (Mezentsev, 2024).

Acknowledgments

The Authors wish to thank Vaisala for the GLD360 lightning detection data, as well as World Wide Lightning Location Network for the WWLLN data. ASIM is a mission of the European Space Agency (ESA) and is funded by ESA and by national grants of Denmark, Norway and Spain. The work of AM is funded through the ASIM Science Data Center and by the Research Council of Norway under the contract 223252/F50 (CoE).

References

- Bjørge-Engeland, I., Østgaard, N., Mezentsev, A., Skeie, C. A., Sarria, D., Lapierre, J., et al. (2022). Terrestrial gamma-ray flashes with accompanying elves detected by ASIM. *Journal of Geophysical Research: Atmospheres*, 127(11), e2021JD036368. <https://doi.org/10.1029/2021JD036368>
- Chanrion, O., Neubert, T., Lundgaard Rasmussen, I., Stoltze, C., Tcherniak, D., Jessen, N. C., et al. (2019). The modular multispectral imaging array (MMIA) of the ASIM payload on the International Space Station. *Space Science Reviews*, 215(28), 28. <https://doi.org/10.1007/s11214-019-0593-y>
- Connaughton, V., Briggs, M. S., Xiong, S., Dwyer, J. R., Hutchins, M. L., Grove, J. E., et al. (2013). Radio signals from electron beams in terrestrial gamma ray flashes. *Journal of Geophysical Research: Space Physics*, 118(5), 2313–2320. <https://doi.org/10.1029/2012JA018288>
- Cummer, S. A., Lu, G., Briggs, M. S., Connaughton, V., Xiong, S., Fishman, G. J., & Dwyer, J. R. (2011). The lightning-TGF relationship on microsecond timescales. *Geophysical Research Letters*, 38(14), L14810. <https://doi.org/10.1029/2011GL048099>
- Cummer, S. A., Lyu, F., Briggs, M. S., Fitzpatrick, G., Roberts, O. J., & Dwyer, J. R. (2015). Lightning leader altitude progression in terrestrial gamma-ray flashes. *Geophysical Research Letters*, 42(18), 7792–7798. <https://doi.org/10.1002/2015GL065228>
- Dwyer, J. R., & Cummer, S. A. (2013). Radio emissions from terrestrial gamma-ray flashes. *Journal of Geophysical Research: Space Physics*, 118(6), 3769–3790. <https://doi.org/10.1002/jgra.50188>
- Hazleton, B. J., Grefenstette, B. W., Smith, D. M., Dwyer, J. R., Shao, X.-M., Cummer, S. A., et al. (2009). Spectral dependence of terrestrial gamma-ray flashes on source distance. *Geophysical Research Letters*, 36(1), 1–5. <https://doi.org/10.1029/2008GL035906>
- Lindanger, A., Skeie, C. A., Marisaldi, M., Bjørge-Engeland, I., Østgaard, N., Mezentsev, A., et al. (2022). Production of terrestrial gamma-ray flashes during the early stages of lightning flashes. *Journal of Geophysical Research: Atmospheres*, 127(8), e2021JD036305. <https://doi.org/10.1029/2021JD036305>
- Lu, G., Blakeslee, R. J., Li, J., Smith, D. M., Shao, X.-M., McCaul, E. W., et al. (2010). Lightning mapping observation of a terrestrial gamma-ray flash. *Geophysical Research Letters*, 37(11), L11806. <https://doi.org/10.1029/2010GL043494>
- Luque, A., Gordillo-Vazquez, F. J., Li, D., Malagon-Romero, A., Perez-Invernón, F. J., Schmalzried, A., et al. (2020). Modeling lightning observations from space-based platforms (CloudScat.jl 1.0). *Geoscientific Model Development*, 13(11), 5549–5566. <https://doi.org/10.5194/gmd-13-5549-2020>
- Mezentsev, A. (2024). Supporting information for “Discerning TGF and leader current pulse in ASIM observation”. <https://doi.org/10.5281/zenodo.11394750>
- Mezentsev, A., Lehtinen, N., Østgaard, N., Perez-Invernón, F. J., & Cummer, S. A. (2018). Spectral characteristics of VLF sferics associated with RHESSI TGFs. *Journal of Geophysical Research: Atmospheres*, 123(1), 139–159. <https://doi.org/10.1002/2017JD027624>
- Østgaard, N., Cummer, S. A., Mezentsev, A., Luque, A., Dwyer, J., Neubert, T., et al. (2021). Simultaneous observations of EIP, TGF, Elve, and optical lightning. *Journal of Geophysical Research: Atmospheres*, 126(11), e2020JD033921. <https://doi.org/10.1029/2020JD033921>
- Østgaard, N., Gjesteland, T., Carlson, B. E., Collier, A. B., Cummer, S. A., Lu, G., & Christian, H. J. (2013). Simultaneous observations of optical lightning and terrestrial gamma ray flash from space. *Geophysical Research Letters*, 40(10), 2423–2426. <https://doi.org/10.1002/grl.50466>
- Østgaard, N., Neubert, T., Reglero, V., Ullaland, K., Yang, S., Genov, G., et al. (2019). First 10 months of TGF observations by ASIM. *Journal of Geophysical Research: Atmospheres*, 124(24), 14024–14036. <https://doi.org/10.1029/2019JD031214>
- Shao, X.-M., Hamlin, T., & Smith, D. M. (2010). A closer examination of terrestrial gamma-ray flash-related lightning processes. *Journal of Geophysical Research*, 115(A6), A00E30. <https://doi.org/10.1029/2009JA014835>
- Skeie, C. A., Østgaard, N., Mezentsev, A., Bjørge-Engeland, I., Marisaldi, M., Lehtinen, N., et al. (2022). The temporal relationship between terrestrial gamma-ray flashes and associated optical pulses from lightning. *Journal of Geophysical Research: Atmospheres*, 127(17), e2022JD037128. <https://doi.org/10.1029/2022JD037128>